Supporting Information For

Arginine-deprivation-induced oxidative damage sterilizes *Mycobacterium tuberculosis*

Sangeeta Tiwari[a, 1], Andries J. van Tonder[b], Catherine Vilchèze[a,c], Vitor Mendes[d], Sherine E. Thomas[d], Adel Malek[a], Bing Chen[a], Mei Chen[a], John Kim[a], Tom L. Blundell[d], Julian Parkhill[b], Brian Weinrick[a], Michael Berney[a] and William R. Jacobs Jr.[a,c,1]

[a]Department of Microbiology and Immunology, Albert Einstein College of Medicine, Bronx, NY 10461
[b]Wellcome Sanger Institute, Wellcome Genome Campus, Hinxton, Cambridge, CB10 1SA, UK
[c]Howard Hughes Medical Institute, Albert Einstein College of Medicine, Bronx, NY 10461
[d]Department of Biochemistry, University of Cambridge, Cambridge CB21GA, UK

[1] Address correspondence to: Phone: (718) 678-1075, E-mail: sangeeta.tiwari@einstein.yu.edu or jacobsw@hhmi.org

Contains:

Supplemental materials and methods

Supplemental References

Supplemental Figures 1-8

Supplemental Tables 1-4

Supplementary Methods

Generation of Allelic exchange substrate (AES) to delete mutants in *Mtb*: Deletion mutants were generated using specialized transduction. To avoid any polar effects we have designed primers to generate in-frame deletions using the strategy described by Jain *et al*., 2014. In collaboration with the Genomics Institute of the Novartis Research Foundation, we generated a set of gene-deletion constructs for *Mtb* and introduced universal uptags and barcodes in primer sequences for Rv1654 and Rv1656 maintaining the frame of the gene. DNA fragments containing ~500 or ~540 bp upstream sequence (LHS) and ~540 or ~544 bp downstream sequence (RHS) were PCR amplified from H37Rv genomic DNA for Rv1654 and Rv1656 respectively. The primer pair used for amplification of upstream sequence (LL-LR) and downstream sequence (RL-RR) is listed in Table S3. PCR products and vector pYUB1471 were digested with Van91I (1). Digestion of pYUB1471 by Van91I released four fragments. Allelic exchange substrate (AES) was constructed by one-step ligation of the two vector fragments (3.6 kb and 1.6 kb), which corresponded to the sacB-hyg cassette, and *oriE-cos* fragment, respectively, with Van91I digested upstream and downstream PCR products (1).

Generation of phasmid and transduction to generate deletion mutants: AES confirmed by sequencing was digested with PacI and ligated into PacI-digested temperature-sensitive phAE159 leading to generation of phasmids phAE773 and phAE 774 (Table S2). Phage were packaged, amplified and transductions were carried out and plated were plated onto 7H10 agar supplemented with 10% OADC enrichment, 0.5% glycerol, 1 mM Arginine (or desired supplement), 0.05% Tween 80, and 75 μg/mL hygromycin B (1). Genomic DNA prepared from hygromycin-resistant colonies was analyzed by three primer PCR (gene_L (P1) + gene_R (P2) + universal uptag (P3)) to confirm gene deletion. Primers were designed in such a way that PCR from the deletion mutant gave a small sized PCR product (gene1_L (P1) + universal uptag (P3)) compared to that from the wild-type (gene1_L (P1)+ gene1_R (P2)) as shown in Fig. S1B and Table S3. Mutants were further confirmed by growth curves in the ± arginine media and by whole-genome sequencing using Illumina MiSeq technology (available upon request). SacB-hyg cassette flanked by γδ-resolvase sites was removed from the deletion mutants by using TM4- derived phage phAE280 expressing the γδ-resolvase enzyme (Table S2). The resulting strains are referred as "unmarked." Transductants were plated on 7H10 medium containing 10% (wt/vol) sucrose, L-arginine (1mM) without hygromycin. Unmarked clones were confirmed by pick and patch on ± 75 μg/mL hygromycin B containing plates and by PCR.

Complementation plasmids and cosmids: For the construction of complemented strains *argB* and *argF* genes were amplified using PCR primers (Table S3). The PCR product was digested with HindIII-HpaI or EcoRI-HpaI and cloned into integrating plasmid pMV361 for generation of pYUB1897 (*argB*) and pYUB1898 (*argF*) respectively (Table S2). Alternatively, as a backup a pYUB1896 cosmid was generated as mentioned in Table S2. pYUB1896, pYUB1897 and pYUB1898 were transformed into unmarked Δ*argB* and Δ*argF* strains by electroporation using standard protocols (2).

Suppressor screen

For screening suppressors, 10^9 bacterial cells of three independent clones of Δ*argB* and Δ*argF* were plated on 7H10-OADC-glycerol plates without additional L-arginine. Plates were checked for colonies after 4 wk and every week for six months.

RNA isolation, microarrays and RNA-Seq: Samples were prepared in triplicate from cultures of H37Rv, Δ*argB,* and Δ*argF* for microarray analysis at days 0, 1, 3, 6 and for RNA-Seq at 0, 4, 48 h during starvation. Cell pellets were suspended in 1ml of Qiagen RNA protect reagent, centrifuged and pellets were suspended in 1 ml Trizol (Life Technologies, Fisher). Suspended cells were lysed using FastPrep-24 and centrifuged. RNA was isolated using Direct-zol RNA miniprep (Zymo Research), followed by preparation of cDNA and microarray analysis was performed as described before (3, 4) using arrays from Microarrays Inc., Gene Expression Omnibus (GEO) platform GPL19545, as previously detailed (3). Transcriptomics data at the different arginine deprivation time points obtained from microarrays were compared to the d 0 (unstarved for arginine) data using T-test volcano plots (Fig. S3*A*) and significance analysis of microarray (SAM) (Fig. S3*B*). Genes that were significantly up- or down-regulated (> 2-fold, P ≤0.05) in both analytical methods were studied further. All the data have been deposited in the Gene Expression Omnibus at NCBI (www.ncbi.nlm.nih.gov/geo) with accession number GSE98821.

For RNA-seq, Ribosomal RNA (rRNA) was depleted from the total extracted RNA using the RiboZero Epidemiology kit (Illumina). Libraries were prepared using TruSeq Stranded RNA Sample Preparation kit (Illumina), checked for quality with the Agilent DNA 1000 kit on a 2100 Bioanalyzer. Sequencing of 75 bp paired-end reads was performed on the Illumina HiSeq 4000 platform. For each sample, sequence reads were mapped against the reference genome *Mycobacterium tuberculosis* H37Rv (v3) using BWA v0.7.15 (5) to produce a BAM file. BWA was used to index the reference and the reads were aligned using default parameters but with the quality threshold for read trimming set to 15 (q=15) and maximum insert size (a) set as the maximum requested fragment size of the sequencing library. Gene expression values were computed from the read alignments to the coding sequencing to generate the number of reads mapping and RPKM (reads per kilobase per million) (6). Only reads with a mapping quality score of 10 were included in the count. Differential expression analyses were performed using wrapper functions from the R package DEAGO 1.0.1 from Pathogen informatics WSI. DESeq2 1.16.1 (7) was used for the normalization of raw counts with default parameters, prior to implementing Wald tests to determine differential expression (alpha = 0.05). Genes with significantly different expression levels were further studied (fold change ≥ 2-fold and P ≤0.05). Heat maps were based on the log2-transformed mean expression values generated by deSEQ2 (7).

TUNEL assay: DNA strand breaks in *Mtb* strains undergoing starvation or H_2O_2 treatment were measured using the in situ cell death detection kit (Roche Molecular Biochemicals, Indianapolis, IN) following manufacturer instructions. DNA strand breaks in *Mtb* strains undergoing starvation or H_2O_2 treatment were labeled using terminal deoxynucleotidyl transferase (TdT), which catalyzes polymerization of fluorescein dUTP to free 3'-OH DNA ends in a template-independent manner. Aliquots of cells from the same cultures used for ROS measurement were removed, washed with PBS buffer, and

fixed in 2% PFA in PBS for 30 min at 25°C and centrifuged. Again, PBS washed cells were permeabilized and stained with TUNEL reaction mix using the *in-situ* cell death detection kit (Roche Molecular Biochemicals, Indianapolis, IN). Samples were labeled for 1 h/37°C in the dark. After labeling, cells were washed with PBS and run on a BD FACS Canto II flow cytometer. Samples were labeled for 1 h/37°C in the dark. After labeling, cells were washed with PBS and stored at 4°C till further analysis. Samples were run on a BD FACS Canto II flow cytometer, and data were acquired using BD FACS Diva software (vs 8.0.1). Data were visualized using the following instrument settings: forward scatter (FSC), 523V log; side scatter (SSC), 478V log. The threshold was set on SSC (1000V). Samples were excited using a laser setting of 488 nm, and emissions were collected using 505 long pass and 525/50 band pass filters. Samples incubated with only label solution without TdT were used as a control, and 10,000 events were acquired for each sample. Single cells positive for TUNEL staining were quantified as percentages of total gated cells.

Hydrogen peroxide killing experiment. *Mtb* strains were grown in 7H9 media supplemented with 1mM L-arginine, to an OD_{600} of 0.5-1.0. Cells were pelleted and washed thrice with PBST. Washed bacteria were diluted to 0.02 OD_{600} in 10 ml 7H9 broth supplemented with 0.2% glycerol, 0.05%, 10% ADS enrichment (50 g albumin, 20 g dextrose, 8.5 g NaCl in 1-liter water) and no L-arginine. After 24h, H_2O_2 (f.c. 16 mM) was added to the cultures for 4 h, followed by plating on L-arginine containing plates to determine cfu (8).

Metabolomics: Bacterial strains were grown to log phase in L-arginine media, washed and transferred to starvation media. 5 ml samples (OD_{600} of 0.5) were quickly quenched in 10 ml methanol at -20°C. Samples were centrifuged at 3300 g/10 min/-9°C. Cell pellets were suspended in 1 ml extraction solvent [40% acetonitrile (vol/vol), 40% methanol (vol/vol), and 20% water (vol/vol)] and transferred to screw-cap tubes containing silica beads. Cells were lysed using the FastPrep-24 (MP Biomedical) twice at 45s/6ms, with incubation of 5 min on ice in-between the cycles. The sample was centrifuged at 1000 rpm/1min/room temperature and 750 µl of the extract was filtered through 0.22 µm Spin-X centrifuge tube filters and frozen at -80°C until analyzed. Samples collected at various time points (days 0, 1, 3 and 6) were analyzed using an Acquity UPLC system (Waters, Manchester, UK) coupled with a Synapt G2 quadrupole-time-of-flight hybrid mass spectrometer using described methods (9, 10). As described previously (9-11) UPLC was performed in a hydrophilic interaction liquid chromatography-mode gradient elution using Acquity 1.7-µm amide column (2.1 × 150 mm). Column eluents were delivered via electrospray ionization. The flow rate was maintained to 0.5 mL/min for both the mobile phase solvents containing 0.1% formic acid, 100% acetonitrile (mobile phase A) and 100% water (mobile phase B). In both positive and negative modes, the gradient was started with 1% B for 1 min, increased to 35% B by 14 min, then 60% B by 17 min, held at 60% B for 1 min, then ramped to 1% B by 19 min and held at 1% B to the end of run at 20 min. The mass spectrometer was operated in V mode for high sensitivity using a capillary voltage of 2 kV and a cone voltage of 17 V. Flow rate and temperature of desolvation gas was kept to 500 L/h and 325 °C while the temperature of the source was 120 °C. MS spectra were acquired in

centroid mode from m/z 50–1,200 with a scan time of 0.5 s. Leucine enkephalin (2 ng/μL) was used as lock mass (m/z 556.2771 and 554.2615 in positive and negative experiments, respectively). All samples were analyzed using MarkerLynx (Waters), which integrates and aligns MS data points and converts them into exact mass retention time pairs to build a matrix composed of retention time, exact mass *m/z,* and intensity pairs. The noise level was 3% in both positive and negative mode. Ions were identified using published databases, and identification was confirmed by comparing retention time accurate mass, and MS/MS data between standards that were commercially available and samples. Fold changes were calculated by comparing metabolite concentration at the respective time to day 0. EZ info (Umetrics, Umea, Sweden) was used for principal component analysis (PCA).

1. Jain P*, et al.* (2014) Specialized transduction designed for precise high-throughput unmarked deletions in *Mycobacterium tuberculosis. MBio* 5(3):e01245-01214.
2. Larsen MH, Biermann K, Tandberg S, Hsu T, & Jacobs WR, Jr. (2007) Genetic Manipulation of Mycobacterium tuberculosis. *Curr Protoc Microbiol* Chapter 10:Unit 10A 12.
3. Vilcheze C, Hartman T, Weinrick B, & Jacobs WR, Jr. (2013) *Mycobacterium tuberculosis* is extraordinarily sensitive to killing by a vitamin C-induced Fenton reaction. *Nat. Commun.* 4:1881-1891.
4. Jain P*, et al.* (2016) Dual-Reporter mycobacteriophages (Phi2DRMs) reveal preexisting *Mycobacterium tuberculosis* persistent cells in human sputum. *MBio* 7(5):e01023-01016.
5. Li H & Durbin R (2010) Fast and accurate long-read alignment with Burrows-Wheeler transform. *Bioinformatics* 26(5):589-595.
6. Mortazavi A, Williams BA, McCue K, Schaeffer L, & Wold B (2008) Mapping and quantifying mammalian transcriptomes by RNA-Seq. *Nat Methods* 5(7):621-628.
7. Love MI, Huber W, & Anders S (2014) Moderated estimation of fold change and dispersion for RNA-seq data with DESeq2. *Genome Biol* 15(12):550-571.
8. Small JL*, et al.* (2013) Perturbation of cytochrome c maturation reveals adaptability of the respiratory chain in *Mycobacterium tuberculosis. MBio* 4(5):1-7.
9. Paglia G*, et al.* (2012) Monitoring metabolites consumption and secretion in cultured cells using ultra-performance liquid chromatography quadrupole-time of flight mass spectrometry (UPLC-Q-ToF-MS). *Anal. Bioanal. Chem.* 402(3):1183-1198.
10. Vilcheze C*, et al.* (2017) Enhanced respiration prevents drug tolerance and drug resistance in *Mycobacterium tuberculosis. Proc Natl Acad Sci U S A* 114(17):4495–4500.
11. Berney M*, et al.* (2015) Essential roles of methionine and S-adenosylmethionine in the autarkic lifestyle of *Mycobacterium tuberculosis. Proc Natl Acad Sci U S A* 112:10008-10013.

Supplementary Figures and legends

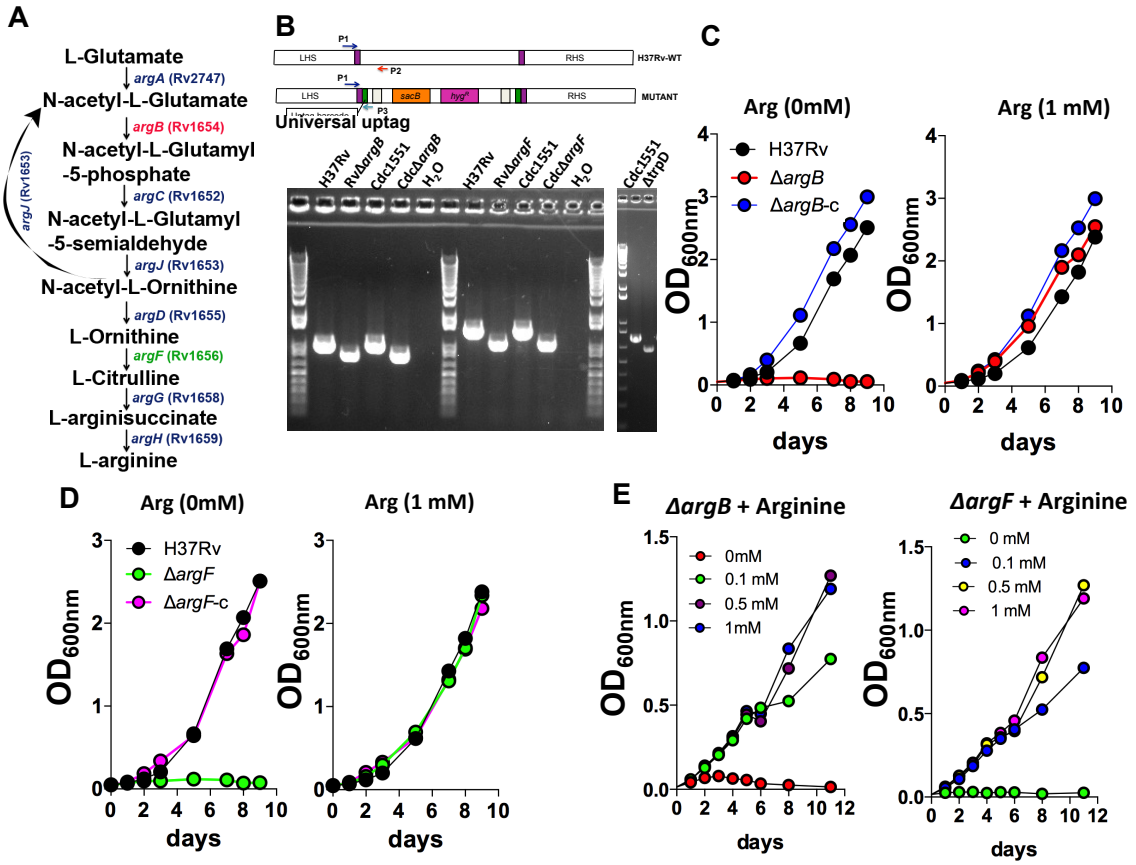

Fig. S1. Construction and characterization of arginine auxotrophic mutants of *Mtb*. Mutants Δ*argB and* Δ*argF*, generated by specialized transduction were confirmed by three-primer PCR and their requirement for arginine supplementation in 7H9 medium. (**A**) Arginine biosynthesis pathway. (**B**) Three-primer PCR. The P2 primer is specific for wild-type strain (H37Rv or CDC1551), the P3 primer is specific for the mutant, and the P1 primer binds to both genomes. (**C**) Growth of H37Rv (black), Δ*argB* (red), and Δ*argB-c* (blue) in 7H9 medium in the absence (left panel) and presence (right panel) of 1 mM L-arginine. (**D**) Growth of H37Rv (black), Δ*argF* (green), and Δ*argF-c* (pink) in the absence (left panel) and presence (right panel) of 1 mM L-arginine. (**E**) The growth of Δ*argB* (left panel) and Δ*argF* (right panel) in 7H9 medium supplemented with different concentrations of L-arginine. Arg: L-arginine.

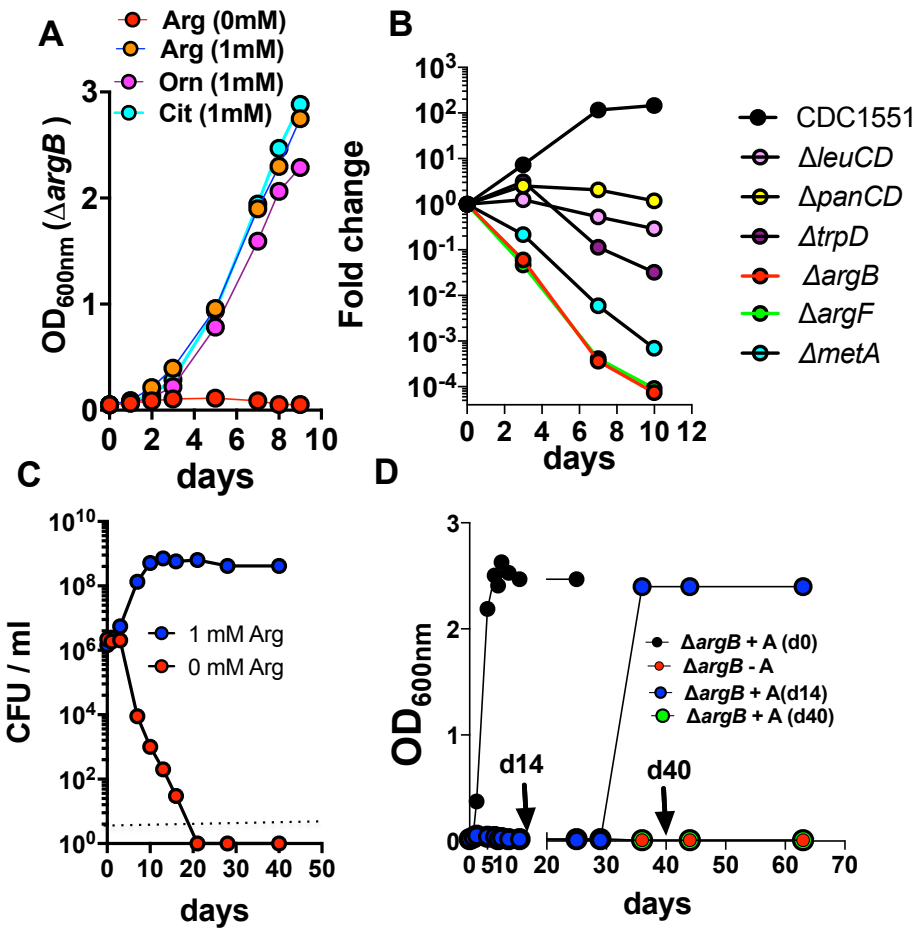

Fig. S2. ArgB is essential for the survival of *Mtb* in the arginine-deprived 7H9 medium. (**A**) Rescue of Δ*argB* with 1 mM of L-arginine or pathway intermediates. Arg, L-arginine; Orn, L-ornithine; Cit, L-citrulline. (**B**) Survival curves of arginine auxotrophic mutants Δ*argB* andΔ*argF,* compared to other auxotrophic mutants of the clinical isolate *Mtb* CDC1551 in 7H9 media lacking respective amino acids or vitamins. For viability determination, samples were plated at indicated time points on media supplemented with the respective amino acids or vitamins. To calculate fold-change in viability, cfu's at indicated time points were compared to cfu's at the zero time point (unstarved), with a fold-change detection limit of $1x10^{-6}$. CDC1551 (wild-type strain), Δ*leuCD* (leucine auxotroph), Δ*panCD* (pantothenate auxotroph), Δ*trpD* (tryptophan auxotroph), Δ*metA* (methionine auxotroph), Δ*argB* and Δ*argF* (arginine auxotrophs). (**C**) Starvation death response of Δ*argB*. The culture of Δ*argB* grown in 7H9 media supplemented with 1mM L-arginine was washed and inoculated at $1x10^{6}$ cfu/ml in the absence (red) or presence (blue) of 1mM L-arginine. The dotted line represents the limit of detection. Growth was assessed, by plating on 7H10 agar plates supplemented with 1mM L-arginine. (**D**) Rescue of Δ*argB* in arginine-deficient 7H9 medium by supplementation with L-arginine "A"(1 mM) at day 0 (black), day 14 (blue), day 40 (green), or no supplementation (red).

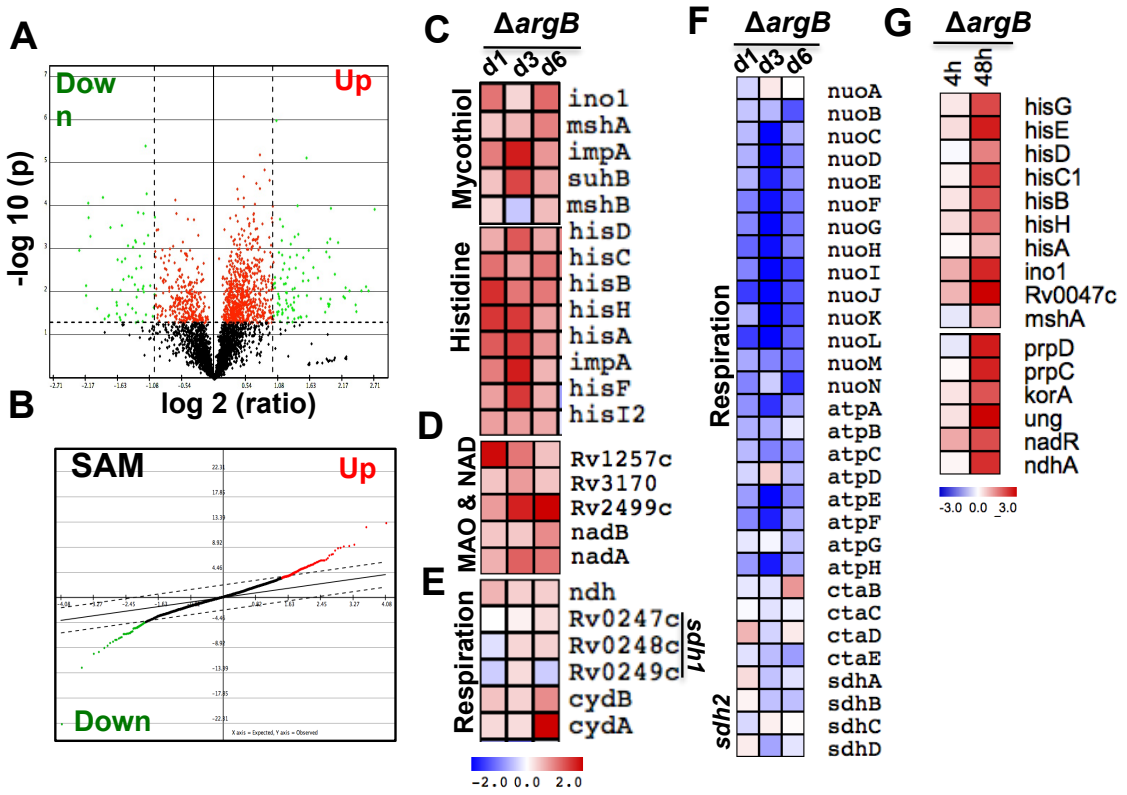

Fig. S3. Kinetics of transcriptomic analysis of Δ*argB* during arginine deprivation. Transcriptomic analysis: (**A-F**) Microarray data; (**G**) RNA-Seq data. (**A**) Volcano plot of the transcriptome of Δ*argB* starved for L-arginine for up to 3 days. Log2 ratios of the fold changes in gene expression were plotted against significance [-log10 (p)]. Dashed black lines and green dots demarcate genes that were up-regulated or down-regulated, respectively, by greater than 2-fold (on the x-axis) with a p-value < 0.05. Genes with no significant change are shown by black dots. Genes with a significant but less than 2-fold change are shown by red dots. (**B**) Significance analysis of microarray (SAM) data for Δ*argB* at early time points (up to day 3) of arginine deprivation. (**C**) Enhanced expression of oxidative stress detoxification thiol systems mycothiol and ergothioneine precursor, histidine. (**D**) Up-regulation of the Fe-S containing enzymes; NAD biosynthesis pathway and monoamine oxidases. (**E**) Up-regulation of alternative respiratory pathways. (**F**) Down-regulation of aerobic (*nuo* and *atp*) respiratory gene clusters. (**G**) RNA-Seq data shows enhanced expression of genes involved in the generation of antioxidant thiols: mycothiol and ergothioneine precursor, myoinositol-1-phosphate and histidine respectively.

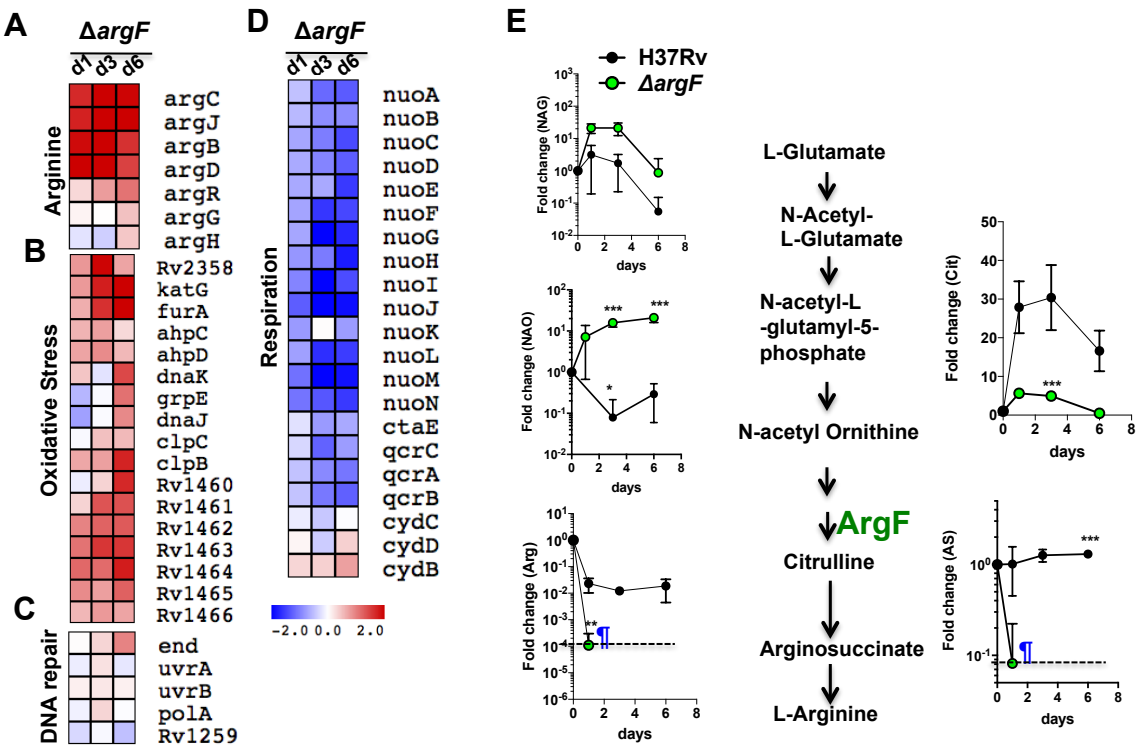

Fig. S4. Kinetics of transcriptomic and metabolomic analysis of Δ*argF*. Time-course transcriptomic and metabolic profile of H37Rv and Δ*argF* during 6 days of arginine deprivation. Samples were harvested at days 0, 1, 3, and 6 from three biologically independent replicates for extraction of RNA and metabolites. (**A-D**) Transcriptomic changes in arginine-deprived Δ*argF* in a time-dependent manner. Up-regulation of genes in the arginine biosynthesis pathway **(A)**, oxidative stress detoxification pathways **(B)** and DNA repair enzymes **(C)**. (**D**) Down-regulation of respiratory gene clusters. All transcriptomic heatmaps show log2-fold changes. (**E**) Metabolomic analysis. Aqueous-phase metabolites were measured by UPLC-MS and fold changes in metabolite abundance were calculated relative to time 0. Results show time-course accumulation of N-acetyl ornithine (NAO) and the upstream metabolite of ArgF and depletion of downstream metabolites L-citrulline (cit), L-arginosuccinate (AS), and L-arginine (Arg). Fold changes are calculated based on metabolite concentration at day 0. Dotted lines represent beyond detection limit. "¶ " Indicates the metabolite was undetectable beyond this time point. **P* < 0.05, ***P* < 0.01, ****P* < 0.001; Students two-tailed t-test.

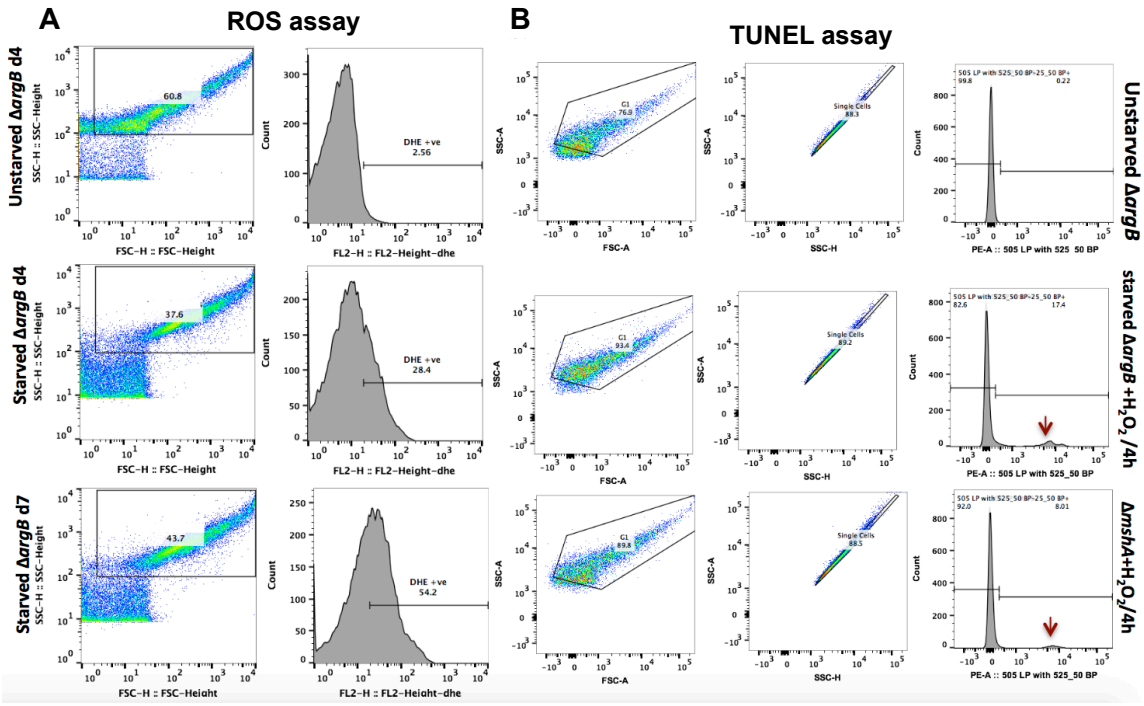

Fig. S5. Arginine unavailability leads to ROS accumulation and DNA damage. Δ*argB* and Δ*argF* were grown in L-arginine-supplemented 7H9 medium, washed and transferred to L-arginine deprived or L-arginine supplemented 7H9 medium. At the indicated time points, cell pellets were collected and were stained (**A**) with dihydroethidium (DHE) for ROS measurement, and (**B**) by TUNEL to measure DNA double-stranded breaks and were analyzed using flow cytometry. **(A)** Gating strategy used to select total and DHE-positive Δ*argB* cells unstarved for L-arginine at day 4 (upper panel), starved for L-arginine at day 4 (middle panel) and day 7 (lower panel). (**B**) Gating strategy used to select total single cell population and percentage of cells undergoing DNA damage as shown by the arrow in starved Δ*argB or* Δ*mshA* at 4h of 16 mM H_2O_2 treatment.

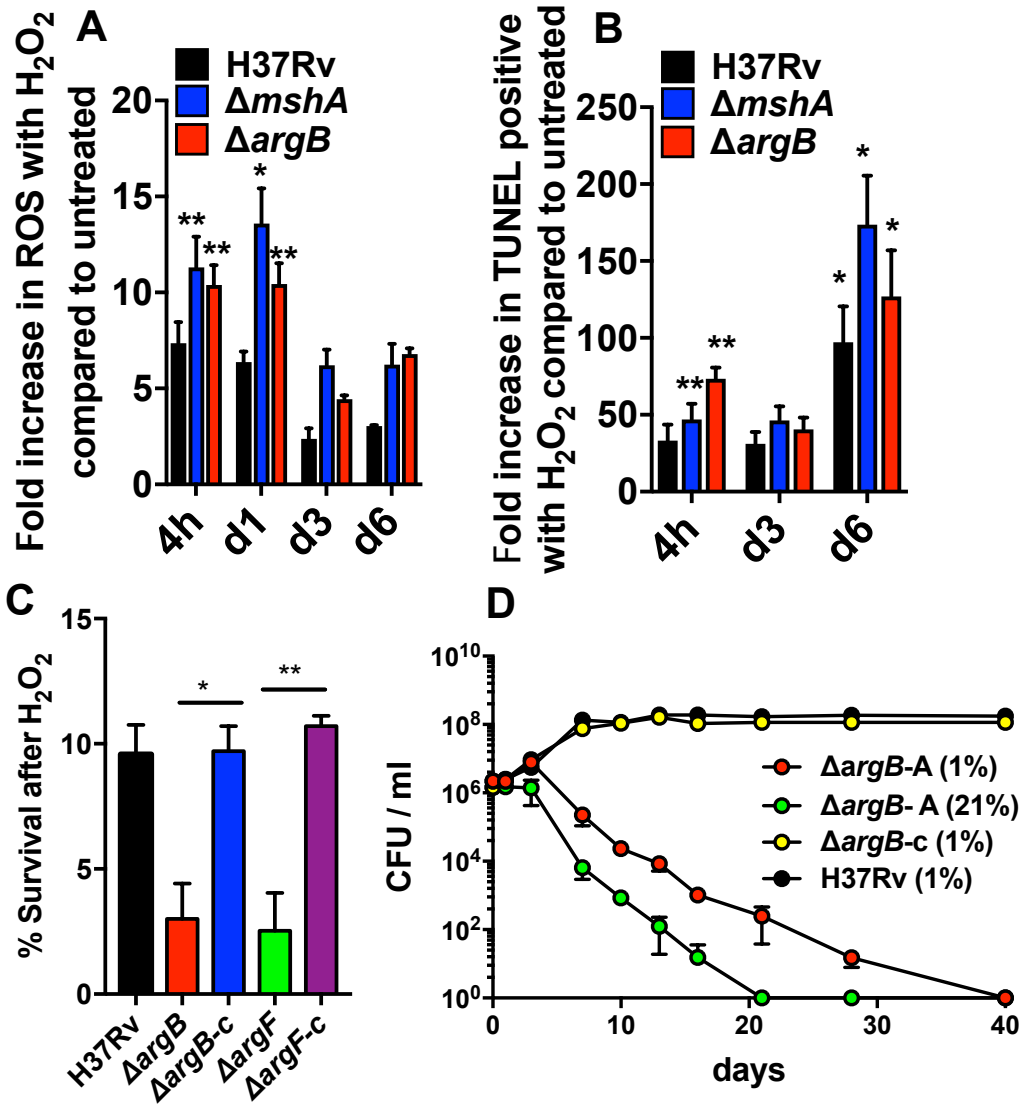

Fig. S6. Arginine deprivation-mediated ROS causes oxidative stress and DNA damage. (**A** and **B**) H37Rv, Δ*argB,* and Δ*mshA* were treated with 16 mM H_2O_2 for 4h, day 1, 3, 6 or left untreated. Levels of (**A**) ROS or (**B**) DNA double-stranded breaks in the H_2O_2-treated samples are shown as fold-change over levels in the untreated samples. Experiments were done in triplicate, and the average with s.d. is plotted. (**C**) Day1 arginine-deprived Δ*argB* and Δ*argF* were exposed for 4h to 16 mM extracellular H_2O_2 to induce oxidative stress. Samples were plated on L-arginine-containing plates to determine cfu's. Average with s.d. is plotted (n = 2). ***$P < 0.001$, **$P < 0.01$, *$P < 0.05$, Student's t-test (two-tailed). (**D**) Strains grown under aerobic conditions were diluted to ~10^6 cells/ml with hypoxic 7H9 media ± L-arginine (1mM). Strains were incubated aerobically (21% O_2 and 5% CO_2) or in a hypoxic chamber (1% O_2 and 5% CO_2). Cultures were plated after 24h to determine day 0 cfu's, followed by plating at indicated time points and were incubated in the aerobic incubator. Experiments were done in duplicates and average ± s.d. is plotted.

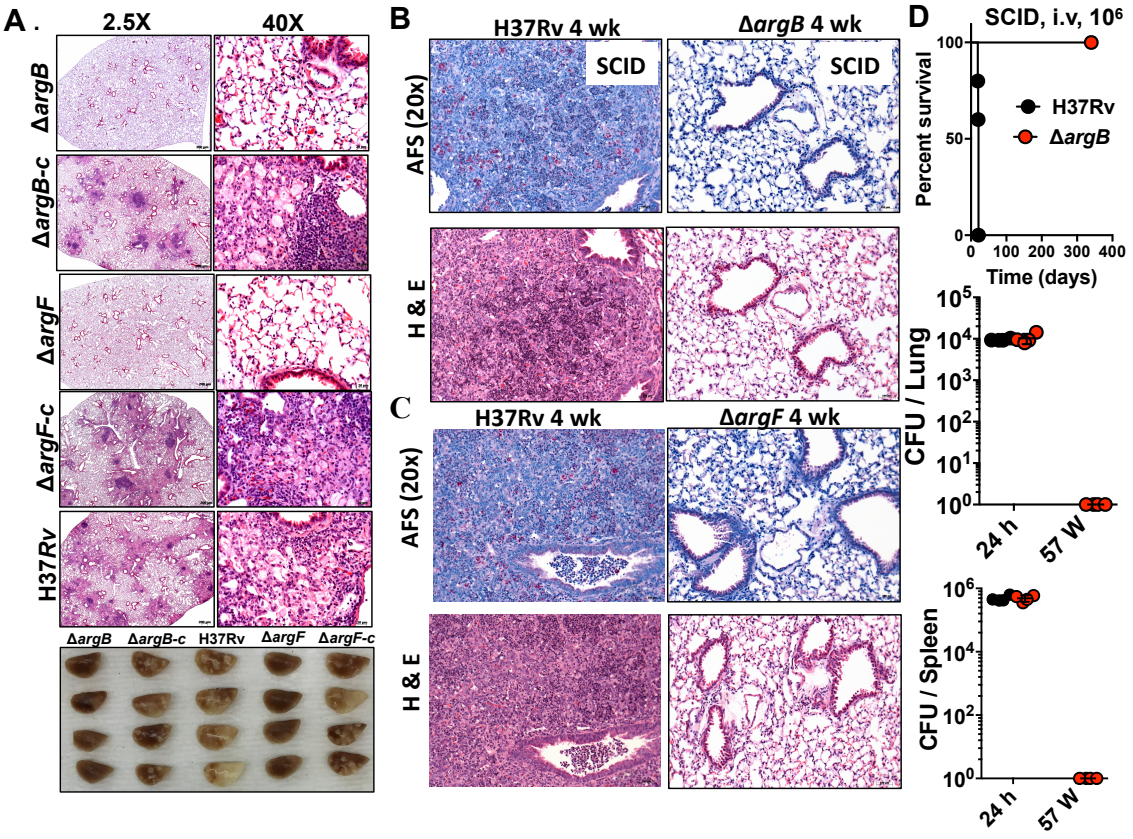

Fig. S7. De novo arginine biosynthesis is required for *Mtb* survival in immunocompetent and immunodeficient mice. Lung histopathology of low-dose aerosol infected (100 bacilli per animal) immunocompetent and immunodeficient mice. (**A**) H&E staining of C57BL/6 mouse lungs at day 28 after infection with the indicated strains; 2.5x and 40x magnification (upper panel), lung gross pathology (lower panel). (**B, C**) Acid-fast staining (AFS) and H&E staining of lungs at 4 wk to detect, respectively, bacilli and infiltrating cells. (**B**) SCID infected with Δ*argB* (right panel) and H37Rv (left panel). (**C**) SCID mice infected with Δ*argF* (right panel) and H37Rv (left panel). (**D**) Δ*argB* gets rapidly sterilized in immunodeficient mice. SCID mice infected i.v. with H37Rv (10^6 bacilli/mice) died in 20-30 days whereas Δ*argB*-infected mice survived > 350 days (Upper panel). Neither Δ*argB* cfu's nor in vivo suppressor mutants (middle and lower panel) were recovered in lungs or spleens at 57 weeks (W) post infection.

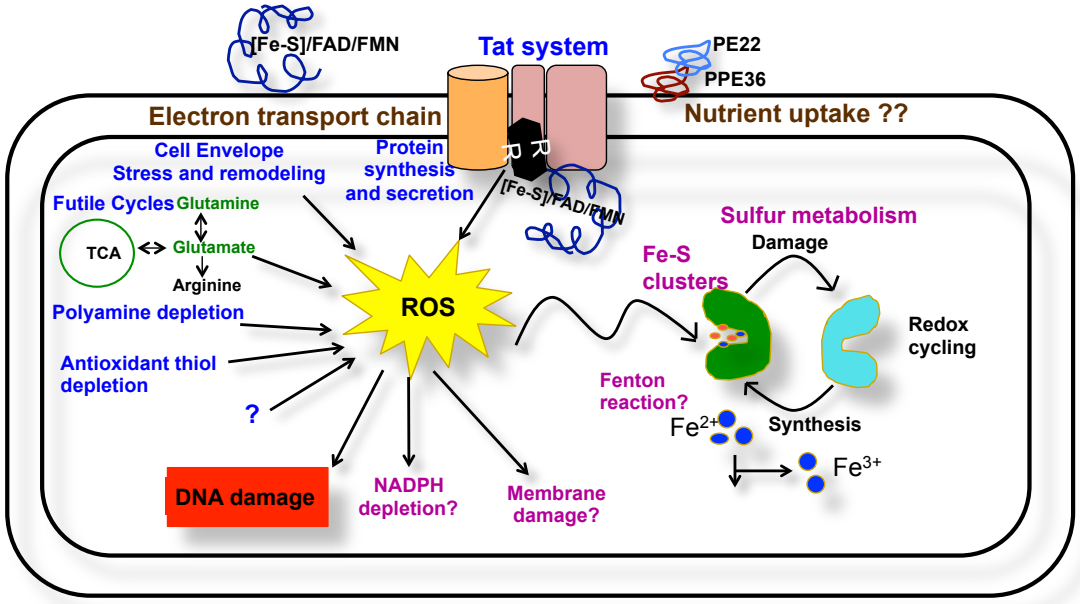

Fig. S8. Schematic representation of the arginine deprivation-mediated, multifactorial death mechanism of the *Mtb*. Futile cycles to generate precursors for arginine biosynthesis, cell envelope stress, depletion of antioxidant thiols and probably polyamines, defective protein synthesis as well as defective secretion of TAT effectors (essential enzymes for nutrition uptake, envelope maintenance and respiration) leads to ROS accumulation and DNA damage leading to *Mtb* cell death.

Table S1: Strains used in the study. Abbreviations used; *kan*^{R}: kanamycin resistance, *hyg*^{R}: hygromycin resistance.

	Strain	Strain no	Genotype	How Constructed	Source/Ref
1	H37Rv (WT)	mc^{2}2	H37Rv wild type	N/A	Trudeau (1)
2		mc^{2}7470	Δ*argB* :: *hyg sacB*	Specialized transduction of H37Rv with phAE773	This Study
3	H37Rv Δ*argB*	mc^{2}7476	Δ*argB*	Specialized transduction of mc^{2}7470 with phAE280	This Study
4	H37Rv Δ*argB-c*	mc^{2}7684	Δ*argB::* pYUB1897 *kan*^{R}	Transformation of mc^{2}7476with pYUB1897 *kan*^{R}	This Study
5		mc^{2}7685	Δ*argB::* pYUB1896 *kan*^{R}	Transformation of mc^{2}7476 with cosmid pYUB1896 *kan*^{R}	This Study
6		mc^{2}8207	Δ*argB* :: pUB1169 *kan*^{R}	Transformation of mc^{2}7476 with pUB1169 *kan*^{R}	This Study
7		mc^{2}7680	Δ*argF* :: *hyg sacB*	Specialized transduction of H37Rv with phAE774	This Study
8	H37Rv Δ*argF*	mc^{2}7958	Δ*argF*	Specialized transduction of mc^{2}7680 with phAE280	This Study
9	H37Rv Δ*argF-c*	mc^{2}7994	Δ*argF::* pYUB1898 *kan*^{R}	Transformation of mc^{2}7958 with pYUB1898 *kan*^{R}	This Study
10		mc^{2}7995	Δ*argF::* pYUB1896 *kan*^{R}	Transformation of mc^{2}7958 with cosmid pYUB1896 *kan*^{R}	This Study
11		mc^{2}8208	Δ*argF* :: pUB1169 *kan*^{R}	Transformation of mc^{2}7958 with pUB1169 *kan*^{R}	This Study
12	CDC1551 Δ*argB*	mc^{2}7477	Δ*argB* (MT1692):: *hyg sacB*	Specialized transduction of CDC1551 with phAE773	This Study
13	CDC1551 Δ*argF*	mc^{2}7681	Δ*argF* (MT1694):: *hyg sacB*	Specialized transduction of CDC1551 with phAE774	This Study
14		mc^{2}8209	H37Rv :: pUB1169 *kan*^{R}	Transformation of H37Rv with pUB1169 *kan*^{R}	This Study
15	Δ*leuCD*	mc^{2}7472	Δ*leuCD*:: *hyg sacB*	Specialized transduction of CDC1551 with phAESP22 Δ*leuCD*	This Study
16	Δ*panCD*	mc^{2}7478	Δ*panCD*:: *hyg sacB*	Specialized transduction of CDC1551 with phAE981 Δ*panCD*	This Study
17	Δ*trpD*	mc^{2}7471	Δ*trpD*:: *hyg sacB*	Specialized transduction of CDC1551 with phAE764 Δ*trpD*	This Study
18	Δ*metA*	mc^{2}7475	Δ*metA*:: *hyg sacB*	Specialized transduction of CDC1551 with phAE778	This Study
19	Δ*mshA*		Δ*mshA*		(1)

1. Vilcheze C, Av-Gay Y, Attarian R, Liu Z, Hazbon MH, Colangeli R, et al. Mycothiol biosynthesis is essential for ethionamide susceptibility in Mycobacterium tuberculosis. Mol Microbiol. 2008;69(5):1316-29.

Table S2. Plasmids and Phasmids. Abbreviations used; *kan*^{R}: kanamycin resistance, *hyg*^{R}: hygromycin resistance, *suc*^{S}: sucrose sensitive, *amp*^{R}*: ampicillin resistance*

	Construct	Description	Reference
1	pMV361	Integrative E. coli *mycobacteria* shuttle vector with hsp60 promoter and *kan*^{R}	[1]
2	pMV261	*aph* oriM P_{hsp60}ColE1; episomal mycobacterial shuttle vector, hsp60 promoter	[1]
3	pYUB412	$attP_{L5}$ λcos int *hyg* bla ColE1; mycobacterial cosmid, integrates into $attB_{L5}$ site of mycobacterial species	S. Bardarov and W.R. Jacobs Jr.
4	pYUB1052	$attP_{L5}$ λcos int aph bla ColE1; derivative of pYUB412; hyg replaced with *kan*^{R}	
5	pYUB1896 *kan*^{R}	pYUB1052, *kan attP$_{L5}$ λcos ColE1* Rv1634-Rv1660 (7B9)	This study
6	pYUB1898	pMV361:: *argF, kan*^{R}	This study
7	pYUB1897	pMV361:: *argB, kan*^{R}	This study
8	phAESP2	Phasmid with flanking regions to delete *panCD* by homologous recombination, *hyg^R, suc^S*	[2]
9	phAESP22	Phasmid with flanking regions to delete *leuCD* by homologous recombination, *hyg^R, suc^S*	[1]
10	phAE764	Phasmid with flanking regions to delete Rv2192c by homologous recombination, *hyg^R, suc^S*	This study
11	phAE778	Phasmid with flanking regions to delete Rv3341 by homologous recombination, *hyg^R, suc^S*	
12	phAE773	Phasmid with flanking regions to delete Rv1654 (*argB)* by homologous recombination, *hyg^R, suc^S*	This study
13	phAE774	Phasmid with flanking regions to delete Rv1656 (*argF)* by homologous recombination, *hyg^R, suc^S*	This study
14	phAE280	Unmarking phage	[1]
15	pHAT4	*E. coli* expression plasmid with N-terminal TEV cleavage site, *amp*^{R}	[3]

1 Jain, P. *et al.* Specialized transduction designed for precise high-throughput unmarked deletions in Mycobacterium tuberculosis. *MBio* **5**, e01245-01214, doi:10.1128/mBio.01245-14 (2014).

2 Sambandamurthy, V. K. *et al.* A pantothenate auxotroph of Mycobacterium tuberculosis is highly attenuated and protects mice against tuberculosis. *Nat Med* **8**, 1171-1174, doi:10.1038/nm765 (2002).

3 Peranen, J., Rikkonen, M., Hyvonen, M. & Kaariainen, L. T7 vectors with modified T7lac promoter for expression of proteins in Escherichia coli. *Anal Biochem* **236**, 371-373 (1996).

Table S3. Primers

AES Construction	
Rv2192c_LL	TTTTTTTTGCATAAATTGCCAGGCCCATCAGGAATGTGA
Rv2192c_LR	TTTTTTTTGCATTTCTTGCGGATACCCTTATGTGACTGTGATG TCTCACTGAGGTCTCTACCGATGCGGCTTCTGCTT
Rv2192c_RL	TTTTTTTTCCATAGATTGGAACCGGAGTCCCTAACGTAACGA GTGTCTGGTCTCGTAGCAGTGCGGCAATCGACACC
Rv2192c_RR	TTTTTTTTCCATCTTTTGGGGCCGTTCAACAGGTCACTG
Rv3341_LL	TTTTTTTTCCATAAATTGGCTTGGTGGCGCAGGGTCT
Rv3341_LR	TTTTTTTTCCATTTCTTGGGAGGAGTATGTAGCTCATCTG ATGTCTCACTGAGGTCTCTCAGCGAGCCGACGTCTATCA
Rv3341_RL	TTTTTTTTGCATAGATTGCGAAACGCCTTAGATATGAGGC GAGTGTCTGGTCTCGTAGTACGGACACGACGGCTTCCT
Rv3341_RR	TTTTTTTTGCATCTTTTGCTCGTCCACTCGACCTGATGG
Rv1654_LL	TTTTTTTTCCATAAATTGGCACCAACGACACCGTGCTG
Rv1654_LR	TTTTTTTTCCATTTCTTGGATACGCATTACCCACAAGGTGAT GTCTCACTGAGGTCTCTAGCACCTGCGCTTTGATGTG
Rv1654_RL	TTTTTTTTCCATAGATTGGGACCCGTATGTTTGGTATAGCGA GTGTCTGGTCTCGTAGCACTGCGTGTTGGTGGAGTTG
Rv1654_RR	TTTTTTTTCCATCTTTTGGCTCTCCCCCATGATCGGTTC
Rv1656_LL	TTTTTTTTCCATAAATTGGGTGCTCGACGAGGTGCAAAC
Rv1656_LR	TTTTTTTTCCATTTCTTGGAGATACCATCCTCCAAAGGTGAT GTCTCACTGAGGTCTCTCGGCTAACCGGGTCTTTCTTC
Rv1656_RL	TTTTTTTTCCATAGATTGGCGTCTCATGCCTGCGTATAGCGA GTGTCTGGTCTCGTAGAGAAGGCGCTGCTGGTGTG
Rv1656_RR	TTTTTTTTCCATCTTTTGGCGGAATAGGCCAGGATGACG
PCR primers for confirmation of deletion mutants of *Mtb*	
Rv3341_L	CAGCTGCTCCGTGACTAC
Rv3341_R	GTCCAGTGATGTGCGAGT
Rv2192c_L	GACATCAGGTTGCGATACTC
Rv2192c_R	GGAGCCTTCATCGTCATC
Rv1654_L	ACCATCACGACAACTGGA
Rv1654_R	GAATCCGCCCTTGAAGTC
Rv1656_L	CGAGTGTTCTTCTGCAACT
Rv1656_R	GCCGAAGTAGGACAACCT
Universal uptag	ATG TCT CAC TGA GGT CTC T
PCR primers for complementation of gene deletions	
pYUB1897: Rv1654_F_HindIII	GCG CTT AAG CTT ATG AGC CGC ATC GAA GCA CTG
pYUB1897: Rv1654_R_HpaI	GCG CTA GTT AAC TCA TCC GCG CAC CAC CTT GGT G
pYUB1898: Rv1656_F_EcoRI	GCGCGCGGAATTCGTGATCAGGCATTTCCTG
pYUB1898: Rv1656_R_HpaI	GTCCAGGTTAACGGCTCATGAGCGCTCCAG

Table S4: Histopathology of Lung sections: H&E and an acid fast stained
Severity scores: 0=no finding; 1=minimal finding; 2=mild finding; 3=moderate finding; 4=marked finding; 5=severe finding
Distribution scores: F = focal; MF = multifocal; D = diffuse

Three mice per group and one section from each mouse were investigated. Numbers represent average of data from 3 mice in each group.

Group	1	2	3	4	5
	SCID mice, 4 weeks				
	H37Rv	Δ*argB*	Δ*argB-c*	Δ*argF*	Δ*argF-c*
Granulomas*	4MF, 3F	0	4MF, 3F	0	3MF, 4F
Necrosis within granulomas	3-4F, 2-3MF	0	4F, 3MF	0	4F, 4MF
Peribronchiolar/ perivascular infiltrates**	2MF	0	2-3MF	0	3MF
Alveolar septal hypercellularity (mixed leukocytes)	3-4D	2-3D	3-4D	3D	3-4D
Acid-fast positive bacilli within inflammatory foci	3-4MF	0	3MF	0	4MF
Atelectasis***	2-3MF	0	2MF	0	2-3MF

* Nodular to diffuse aggregates of macrophages +/- neutrophils, lymphocytes
** Infiltrates include lymphocytes, plasma cells, histiocytes
*** Unclear if the atelectasis is a true lesion or due to post mortem handling-associated damage